

# Fuzzy PID-Based Trajectory Control for a 5-DoF Robot with Disturbance Compensation and Simscape Integration

Thi-Van-Anh Nguyen<sup>1</sup>, Van-Thien Sam<sup>1</sup>, Xuan-Hiep Nguyen<sup>1</sup>, Ngoc-Son Nguyen<sup>1</sup>, Hoang-Viet Dang<sup>1</sup> and Danh-Huy Nguyen<sup>1,\*</sup>

<sup>1</sup>*School of Electrical and Electronic Engineering, Hanoi University of Science and Technology, Hanoi 100000, Vietnam*

\**Corresponding author: huy.nguyendanh@hust.edu.vn*

---

## Abstract

This paper presents a study on the trajectory tracking control of a 5-DoF robot using a Fuzzy PID controller. The robot's kinematic and dynamic models were developed, with specifications detailed for its components, including dimensions, weight, and joint angles. A Fuzzy PID controller was implemented to dynamically adjust control parameters based on error feedback and its derivative. The simulations demonstrated the controller's efficacy in minimizing angular and positional errors, achieving high accuracy and stability. The system's robustness was further evaluated under disturbance conditions, showcasing the controller's effectiveness in maintaining trajectory accuracy. Additionally, simulations were performed in Simscape to simulate the physical environment of the robot. The results indicate that the proposed Fuzzy PID controller significantly enhances the robot's capability to follow desired trajectories, ensuring reliable and precise operation in various environments.

**Keywords:** 5-DoF Robot, Fuzzy PID Control, Trajectory Tracking, Kinematic Modeling, Membership function.

---

## 1. Introduction

With the rapid advancement of science and technology, robotics has seen remarkable growth and significant milestones [1], [2], [3], [4], [5]. Robots provide high precision, flexibility, and enhanced capabilities in numerous applications, from industrial automation to research and development. These robots enhance precision in tasks requiring fine motor control, improve operational efficiency, and reduce human involvement in dangerous or complex environments. As the demand for advanced robotic systems increases, the need for reliable control strategies also becomes crucial [6], [7], [8]. One promising approach to improving robot performance is the implementation of Fuzzy PID controllers.

Traditional PID controllers are widely used in industrial applications due to their simplicity and effectiveness [9], [10], [11], [12]. However, they may not always provide the required performance in highly dynamic and uncertain environments. Fuzzy logic controllers can handle uncertainties and nonlinearities more effectively by mimicking human reasoning and decision-making processes. By combining the strengths of both approaches, Fuzzy PID controllers offer a robust solution for precise and adaptable control in robotics with various implementations [13], [14], [15], [16]. In order to dynamically compute the settings of a PID controller, article [17] presented a convincing method in which fuzzy rules were built based on the errors and rates of error change. This approach simplified the control process by significantly avoiding the complications related to kinematic difficulties. The authors demonstrated how these fuzzy rules improve the control system's accuracy and flexibility in a variety of scenarios by efficiently adjusting the PID settings in real-time. Meanwhile, another significant study detailed in research [18] proposed an innovative tech-

nique for implementing Fuzzy PID controllers using the pole placement method. This approach meticulously separates the evaluation processes for the fuzzy controller and the traditional fixed-parameter PID controller. By doing so, the research highlights the improved performance and robustness of the control system when leveraging the strengths of both fuzzy logic and conventional PID control techniques. The study provides insightful comparisons and practical evaluations, underscoring the benefits of this hybrid approach in achieving superior control accuracy and efficiency. These advancements in Fuzzy PID control represent a significant leap forward in control systems, offering enhanced flexibility and resilience in diverse applications. In particular, these controllers have achieved notable success in managing multi-degree-of-freedom robotic systems, significantly enhancing precision and performance in various tasks [19], [20], [21], [22].

This paper focuses on the implementation of a Fuzzy PID controller for a robot with 5 degrees of freedom (5-DoF), aiming to enhance precision and stability. The Fuzzy PID controller combines the advantages of fuzzy logic and traditional PID control, dynamically adjusting control parameters based on real-time error feedback and its derivative. This approach not only improves the accuracy of trajectory tracking but also enhances the system's adaptability in complex environments. By effectively handling uncertainties and nonlinearities, the Fuzzy PID controller provides a robust, flexible, and reliable solution, paving the way for the widespread adoption of advanced robotic systems.

Initially, the kinematic and dynamic models of the robot are developed. The kinematic model includes detailed specifications of the robot's components, such as dimensions, weight, joint angles, and maximum velocities. These specifications are crucial for understanding the robot's physical and operational

characteristics, which directly impact its performance. The dynamic model encompasses the forces and moments required for joint movements, providing a comprehensive framework for designing effective control algorithms. The design and implementation of the Fuzzy PID controller are then presented. The controller's structure, membership functions, and control rules are thoroughly described, illustrating how the system adapts to varying conditions during operation. The fuzzy inference system, which interprets the input variables and adjusts the control parameters, plays a central role in enhancing the robot's responsiveness and precision. The simulations are conducted to evaluate the performance of the proposed controller in minimizing angular and positional errors. The simulations test the robot's ability to follow desired trajectories, including both straight and curved paths. The results demonstrate the controller's efficacy in achieving high precision and stability. In addition, disturbance was introduced to assess the robustness of the Fuzzy PID controller under challenging conditions, where it effectively maintained accurate trajectory tracking. The simulations were further extended in Simscape, providing a realistic physical environment for evaluating the robot's dynamic response and control performance.

The key contributions of this paper include:

- The paper presents a Fuzzy PID controller that enhances both precision and robustness in trajectory tracking for a 5-DoF robot, maintaining stability and accuracy even under disturbance conditions.
- The use of Simscape simulations provides a realistic evaluation of the robot's dynamic behavior, strengthening the validation of the control strategy.

The structure of this paper is organized as follows: Section 2 presents the modeling of the 5-DoF robot, detailing its specifications, kinematic, and dynamic models. Section 3 focuses on the design and implementation of the Fuzzy PID controller, including its structure, membership functions, and control rules. Section 4 provides the simulation results, demonstrating the performance of the Fuzzy PID controller in minimizing angular and positional errors during trajectory tracking. Finally, the conclusions are discussed in Section 5.

## 2. Modeling the 5-DoF Robot

### 2.1. Robot's specifications

The robot's specifications are comprehensively detailed in Table 1 and Table 2. These tables provide critical information regarding the dimensions, weight, joint angles, and maximum velocities of the robot's components, ensuring a thorough understanding of its physical and operational characteristics.

**Table 1:** Dimensions and Weight Specifications

Component	Length (mm)	Weight (kg)
Base	350	2.6
Link 1	310	2.2
Link 2	380	3
Link 3	200	1.6

**Table 2:** Joint Angles and Maximum Velocity Specifications

Joint	Maximum angular position	Maximum angular velocity
$J_1$	$-35^\circ - 215^\circ$	$200^\circ/\text{s}$
$J_2$	$-50^\circ - 50^\circ$	$220^\circ/\text{s}$
$J_3$	$-160^\circ - 90^\circ$	$180^\circ/\text{s}$
$J_4$	$-180^\circ - 180^\circ$	$270^\circ/\text{s}$
$J_5$	$-180^\circ - 180^\circ$	$200^\circ/\text{s}$

### 2.2. Forward Kinematics Model

Figure 1 illustrates the coordinate system of the robot. This coordinate system forms the basis for defining the robot's kinematics and dynamics.

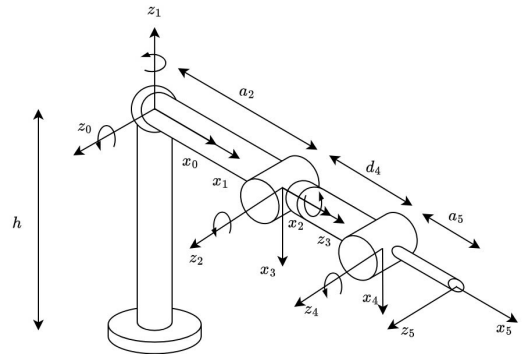


**Figure 1:** The coordinate system of the robot

From the coordinate system 1, we construct the D-H table as shown in Table 3, through which we build the homogeneous transformation matrices  $A_i$ .

Link	$\theta_i$	$d_i$	$a_i$	$\alpha_i$
1	$\theta_1$	0	0	$-\pi/2$
2	$\theta_2$	0	$a_2$	$\pi/2$
3	$\theta_3 - \pi/2$	0	0	$-\pi/2$
4	$\theta_4$	$d_4$	0	$\pi/2$
5	$\theta_5 + \pi/2$	0	$a_5$	0

**Table 3:** D-H Parameters

Where:

$\theta_i$ : The angle of rotation around the axis  $z_{i-1}$  such that the axis  $x_{i-1}$  aligns with the axis  $x_i$ .

$d_i$ : The distance between the axes  $x_{i-1}$  and  $x_i$  along the direction of the axis  $z_{i-1}$ .

$a_i$ : The distance between the axes  $z_{i-1}$  and  $z_i$  along the direction of the axis  $x_i$ .

$\alpha_i$ : The angle of rotation of the axis  $x_i$  to align the axis  $z_{i-1}$  with the axis  $z_i$ .

$$A_i = \begin{bmatrix} \cos \theta_i & -\sin \theta_i \cdot \cos \alpha_i & \sin \theta_i \cdot \sin \alpha_i & a_i \cdot \cos \alpha_i \\ \sin \theta_i & \cos \theta_i \cdot \cos \alpha_i & -\cos \theta_i \cdot \sin \alpha_i & a_i \cdot \sin \alpha_i \\ 0 & \sin \alpha_i & \cos \alpha_i & d_i \\ 0 & 0 & 0 & 1 \end{bmatrix} \quad (1)$$

When the transformation matrices between successive coordinate systems are obtained, the transformation matrix between

the base and the end-effector of the robot can be determined by multiplying these matrices from 1 to 5:

$$T_5^0 = A_1.A_2.A_3.A_4.A_5 = \begin{bmatrix} n_x & o_x & a_x & p_x \\ n_y & o_y & a_y & p_y \\ n_z & o_z & a_z & p_z \\ 0 & 0 & 0 & 1 \end{bmatrix} \quad (2)$$

### 2.3. Inverse Kinematics Model

In the forward kinematics problem, the position and orientation of the end-effector are determined from the known joint variables. To control the robot, forces or moments are applied to the joint variables rather than directly controlling the end-effector. To ensure the robot moves along the desired trajectory, the inverse kinematics problem must be solved to determine the joint variables corresponding to the position and orientation of the end-effector.

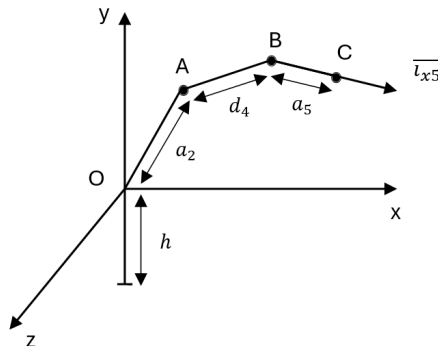


Figure 2: The robot on the original coordinate system

Based on matrix 2 and Figure 2, we obtain the coordinates of the end-effector point  $C(p_x; p_y; p_z)$  and the coordinates of point  $B(x_B; y_B; z_B)$ :

$$x_B = p_x - a_5 n_x, \quad y_B = p_y - a_5 n_y, \quad z_B = p_z - a_5 n_z.$$

The coordinates of point B correspond to the position and orientation of the coordinate frame 4. Through matrix transformations and using Matlab, the joint angles of the robot can be determined.

### 2.4. Dynamics Model

For the robot to move, the actuators must generate sufficient forces or moments to move the joints. The dynamic equations calculate these forces and moments, showing their relationship with position, velocity, and acceleration. Solving these equations allows the determination of acceleration, velocity, and position from the applied forces or moments. The dynamic equations also assist in designing the robot's control system by calculating the kinetic, potential energy, and required moments for the joints.

The structure of the robot is shown below:

where:

$m_i$ : mass of link i.

$j_i$ : moment of inertia of link i with respect to the axis through the center of mass of the link.

$l_i$ : length of link i.

$l_{gi}$ : length from joint i to the center of link i.

$\theta_{ai}$ : rotation angle of link i.

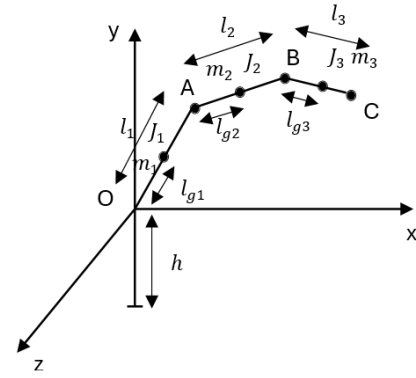


Figure 3: Robot structure

The structure of the robot is shown below:

$$L = K - P = K_1 + K_2 + K_3 - P_1 - P_2 - P_3 \quad (3)$$

The moments for the 5 joints are calculated using the formula:

$$M_i = \frac{d}{dt} \left( \frac{\partial L}{\partial \dot{\theta}_i} \right) - \frac{\partial L}{\partial \theta_i} \quad (4)$$

Substituting 3 into 4, we obtain the moments of the 5 joints in implicit form using Matlab. The dynamic equation can be written in matrix form as follows:

$$\bar{M} = M(\bar{q})\ddot{\bar{q}} + C(\bar{q}, \dot{\bar{q}}) + G(\bar{q}) \quad (5)$$

$$\text{where } M = \begin{bmatrix} M_{11} & M_{12} & M_{13} & M_{14} & M_{15} \\ M_{21} & M_{22} & M_{23} & M_{24} & M_{25} \\ M_{31} & M_{32} & M_{33} & M_{34} & M_{35} \\ M_{41} & M_{42} & M_{43} & M_{44} & M_{45} \\ M_{51} & M_{52} & M_{53} & M_{54} & M_{55} \end{bmatrix}, \quad C^T = [C_1 \quad C_2 \quad C_3 \quad C_4 \quad C_5], \quad G^T = [g_1 \quad g_2 \quad g_3 \quad g_4 \quad g_5].$$

Where:

M: The component of moment of inertia.

C: The component of torque caused by viscous friction and centrifugal force.

G: The component of torque caused by gravitational force.

The matrix values are too complex and lengthy to display in full. Let  $s_i = \sin(\theta_i)$  and  $c_i = \cos(\theta_i)$  for  $i = 1, 2, 3, 4, 5$ , where  $\theta_i$  are the joint angles of the robot. Below are some representative components:

$$M_{44} = \frac{m_3}{2} \left\{ \frac{a_5^2}{2} \left[ (c_1 c_4 s_2 s_5 + c_3 s_1 s_4 s_5 + c_1 c_2 s_3 s_4 s_5)^2 + (c_4 s_1 s_2 s_5 - c_1 c_3 s_4 s_5 + c_2 s_1 s_3 s_4 s_5)^2 + (c_2 c_4 s_5 - s_2 s_3 s_4 s_5)^2 \right] - \frac{j_3 (c_1 c_4 s_2 s_5 + c_3 s_1 s_4 s_5 + c_1 c_2 s_3 s_4 s_5)^2}{(c_5 s_1 s_3 - c_1 c_2 c_3 c_5 + c_3 c_4 s_1 s_5 - c_1 s_2 s_4 s_5 + c_1 c_2 c_4 s_3 s_5)^2 - 1} \right\}$$

$$g_4 = \frac{a_5 g m_3 (c_4 s_1 s_2 s_5 - c_1 c_3 s_4 s_5 + c_2 s_1 s_3 s_4 s_5)}{2}.$$

## 3. Design of the Fuzzy PID Controller for the 5-DoF Robot

### 3.1. Diagram and Structure of the Fuzzy PID Controller

The control diagram of the robot is shown in Figure 4. In the Fuzzy PID controller, the parameters  $K_p$ ,  $K_i$ , and  $K_d$  are

dynamically adjusted based on fuzzy inference rules from the error  $E(t)$  and the derivative of the error  $De(t)$ . These rules determine the change in  $K_p$ ,  $K_i$ , and  $K_d$  according to the system state.

The output of the PID controller is also the output of the FPID (Fuzzy Proportional Integral Derivative) controller, including control signals adjusted by the Fuzzy controller. After  $K_p$ ,  $K_i$ , and  $K_d$  parameters are adjusted, they are used in the PID controller to generate the final control signal, ensuring the system operates smoothly.

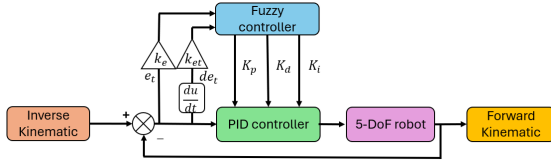
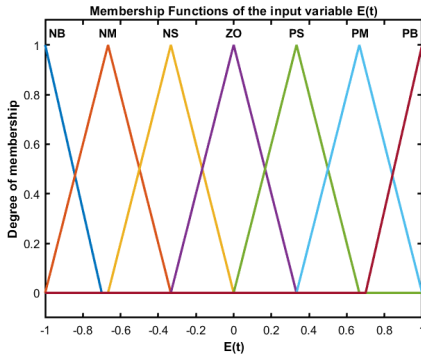


Figure 4: Structure of Fuzzy-PID controller

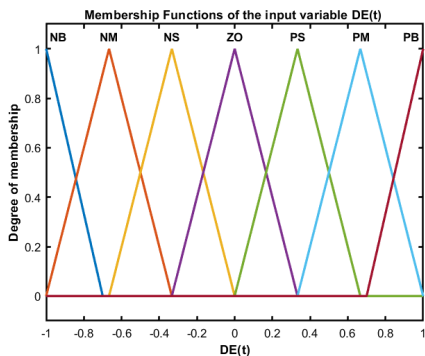
### 3.2. Membership Functions

With the input linguistic variables  $E(t)$  and  $De(t)$  and output variables  $K_p$ ,  $K_d$ ,  $K_i$ , we construct the values of the linguistic variables as follows: NB (Negative Big), NM (Negative Medium), NS (Negative Small), ZE (Zero), PS (Positive Small), PM (Positive Medium), PB (Positive Big).

Using these values, the membership functions are constructed based on the PID parameters calculated above, as shown in figures 5 and 6 of the first angle.



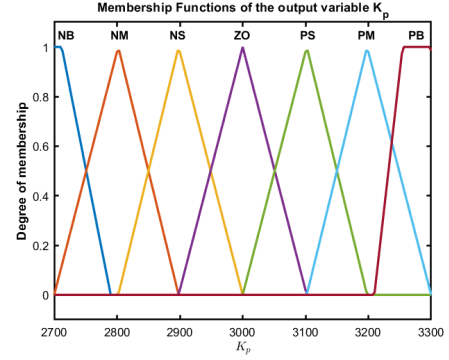
(a) Membership function for the input variable  $E(t)$



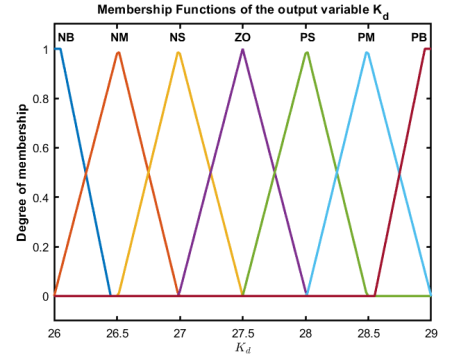
(b) Membership function for the input variable  $De(t)$

Figure 5: Membership function for the input variables

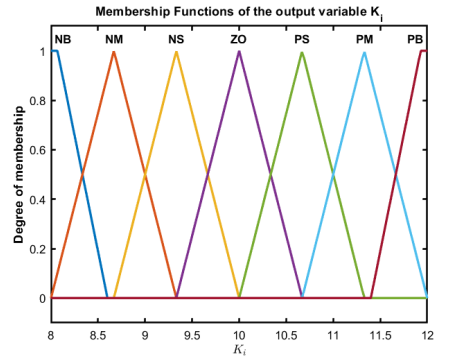
To control the 5 joints of the robot, we need to use 5 Fuzzy PID controllers, with similar input variables and membership



(a) Membership function for the out variable  $K_p$ .



(b) Membership function for the out variable  $K_d$ .



(c) Membership function for the out variable  $K_i$ .

Figure 6: Membership function for the out variables of the first joint

functions. The difference lies in the three outputs  $K_p$ ,  $K_d$ ,  $K_i$  of each controller. Each of these controllers is designed to adjust one joint of the robot, based on the deviation between the actual position and the desired position of the joint, along with the derivative of the deviation, to map to the control values  $K_p$ ,  $K_d$ ,  $K_i$ . These values are adjusted differently between the controllers to ensure each joint is optimally and accurately controlled, according to the specific characteristics of each joint.

### 3.3. Control Rules

As mentioned, the robot uses 5 FPID controllers to control 5 angles, with similar structures and control rules. The control rules are shown in Table 4, Table 5, and Table 6.

The creation of the fuzzy controller mostly depends on using expert knowledge to determine the defuzzification and composition rules. The fuzzy logic system's foundation is made up of these principles, which convert practical observations into workable control schemes. Several simulations are run

during this calibration phase to see how parameter changes affect the system's functionality. The development team may determine ideal parameters that reduce departures from the intended trajectory by closely examining the mistakes that arise from these simulations. Continuous improvement is made possible by this iterative process, which guarantees that the fuzzy controller effectively adjusts to changing circumstances. In the end, the inferences made from these simulation findings result in a fuzzy controller that is reliable and precisely calibrated. A thorough framework for creating a controller that can manage real-world uncertainties and ensure accurate, dependable performance is provided by the knowledge gathered from professional experience as well as thorough testing and calibration.

**Table 4:** Fuzzy rules of  $K_p$

$d_{ek} \setminus e_k$	NB	NM	NS	ZO	PS	PM	PB
NB	PB	PM	NM	NM	NM	NS	PS
NM	PB	PM	NM	NS	NS	NS	ZO
NS	ZO	NS	NS	NB	NM	NS	ZO
ZO	ZO	NM	NM	NM	NM	NS	ZO
PS	ZO	ZO	ZO	ZO	ZO	ZO	ZO
PM	PB	NM	PM	PM	PS	PS	PM
PB	PB	PB	PM	PS	PS	PS	PM

**Table 5:** Fuzzy rules of cho  $K_d$

$d_{ek} \setminus e_k$	NB	NM	NS	ZO	PS	PM	PB
NB	PS	PM	PB	PM	PS	ZO	ZO
NM	PS	PM	PM	PM	PS	ZO	NS
NS	PB	PM	PS	ZO	NS	NS	NS
ZO	PB	PM	PS	NS	NS	NS	NM
PS	PM	PS	ZO	NS	NM	NM	NS
PM	PS	ZO	NS	NS	NS	NM	NB
PB	ZO	ZO	NS	NS	NM	NM	NB

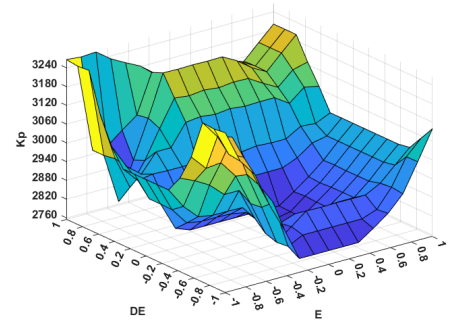
**Table 6:** Fuzzy rules of  $K_i$

$d_{ek} \setminus e_k$	NB	NM	NS	ZO	PS	PM	PB
NB	NB	NM	NM	NS	NS	NS	ZO
NM	NB	NM	NS	NS	ZO	ZO	ZO
NS	NM	NM	NS	ZO	ZO	PS	PM
ZO	NB	NM	NS	ZO	PS	PM	PB
PS	NM	NS	ZO	PS	PM	PM	PB
PM	NM	NS	PS	PM	PM	PB	PB
PB	ZO	ZO	PS	PS	PM	PM	PB

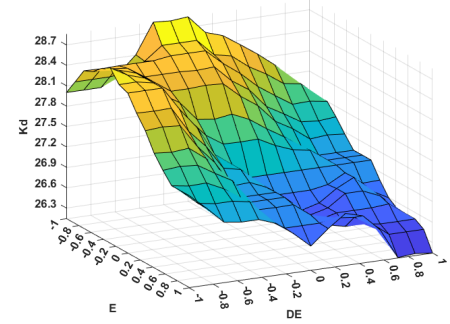
The surface illustrates the relationship between the input and output  $K_p$  in Figure 7a,  $K_d$  in Figure 7b, and  $K_i$  in Figure 7c of the fuzzy controller, highlighting how changes in the input variables influence the output.

## 4. Simulation results

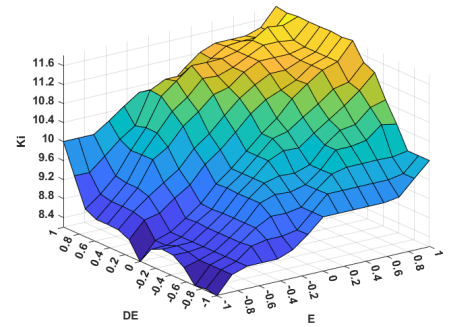
The simulation results demonstrate the responses of the angles to the proposed control inputs, highlighting the performance and accuracy of the Fuzzy PID controller in tracking the desired trajectories. Figure 8 shows the kinematic model of the 5-DOF robot in Simscape, used to analyze the robot's motion and control behavior.



(a) Surface showing the relationship between the input and output  $K_p$ .



(b) Surface showing the relationship between the input and output  $K_d$ .



(c) Surface showing the relationship between the input and output  $K_i$ .

**Figure 7:** Surface showing the relationship between the input and output variables of the fuzzy controller

The kinematic model of a figure 8 configuration with inputs 1, 2, 3, 4, and 5 represents the torques provided to the corresponding joints of the robot. The output of the model gives the angular positions of the joints after applying the torques.

### 4.1. Tracking desired trajectory without disturbance

The simulation results include comparisons and errors for various angles and the end-effector without disturbance. Figure 9 provides the comparison of the actual and reference values for the end-effector.

The errors for each joint angle and the end-effector are illustrated in the following figures. Figure 10 shows the error of the end-effector, while Figure 11a depicts the error of the first angle. Similarly, Figure 11b presents the error of the second angle, Figure 11c illustrates the error of the third angle, Figure 11d shows the error of the fourth angle, and finally, Figure 11e

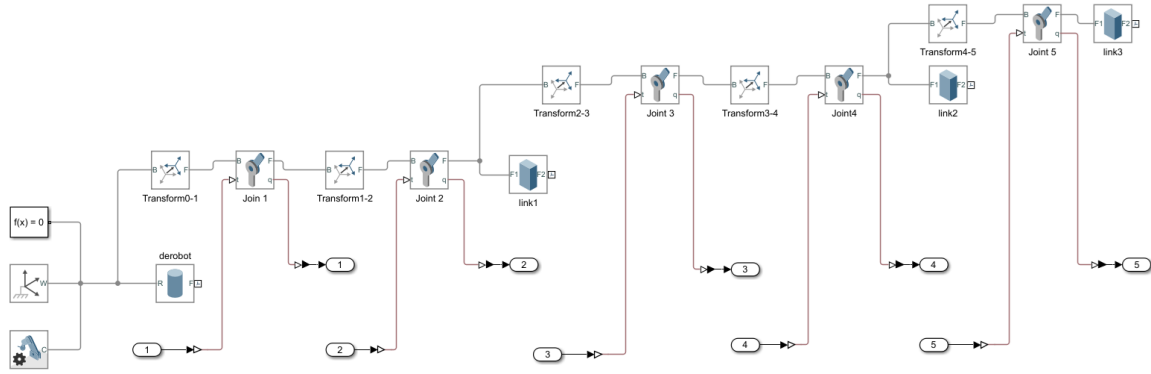


Figure 8: Kinematic Model of a 5-DOF Robot in Simscape

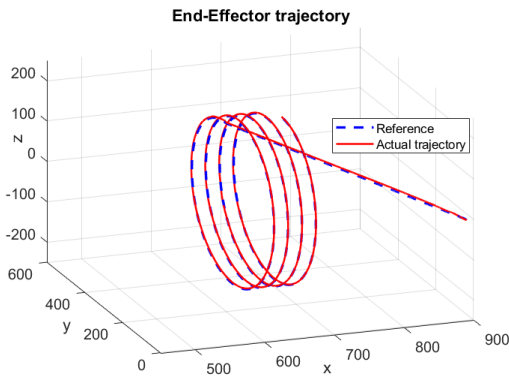


Figure 9: Comparison of actual and reference value for end-effector

highlights the error of the fifth angle.

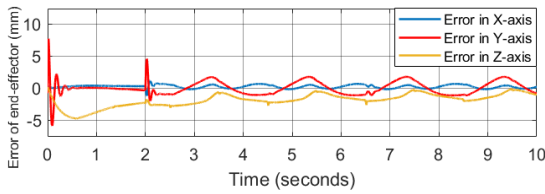
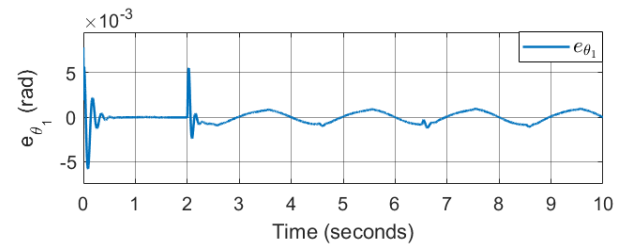


Figure 10: Error of end-effector

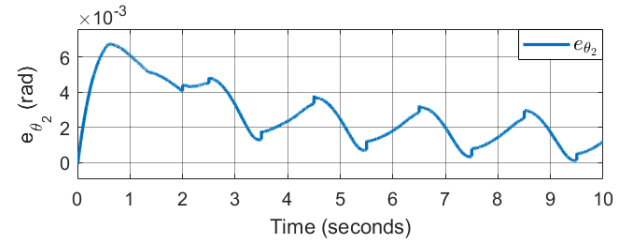
Table 7: RMS and Max errors for tracking without noise

$e$	Max Error	RMSE
$e_{\theta_1} (rad)$	$7.822 \times 10^{-3}$	$9.115 \times 10^{-4}$
$e_{\theta_2} (rad)$	$6.748 \times 10^{-3}$	$3.608 \times 10^{-3}$
$e_{\theta_3} (rad)$	$9.243 \times 10^{-3}$	$1.743 \times 10^{-3}$
$e_{\theta_4} (rad)$	$7.084 \times 10^{-3}$	$1.059 \times 10^{-3}$
$e_{\theta_5} (rad)$	$1.214 \times 10^{-2}$	$3.950 \times 10^{-4}$
$e_{x-axis} (mm)$	1.22	$3.373 \times 10^{-1}$
$e_{y-axis} (mm)$	7.682	1.161
$e_{z-axis} (mm)$	4.787	2.421

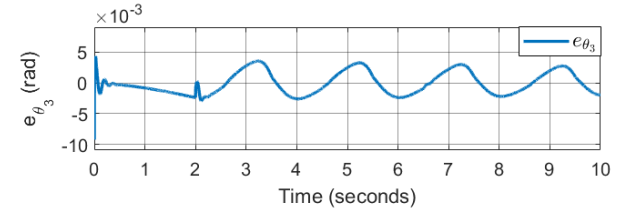
Table 7 demonstrates low angular tracking errors, with  $e_{\theta_5}$  exhibiting the smallest RMSE ( $3.950 \times 10^{-4}$  rad) and the largest maximum error ( $1.214 \times 10^{-2}$  rad). Positional errors are similarly well-controlled, particularly along the  $x$ -axis, which shows the smallest maximum error (1.22 mm). Overall, these results highlight the system's high accuracy in both angular and positional tracking in the absence of noise.



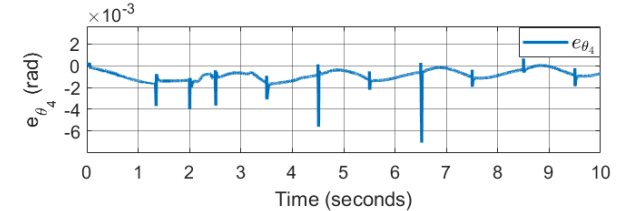
(a) Error of the first angle



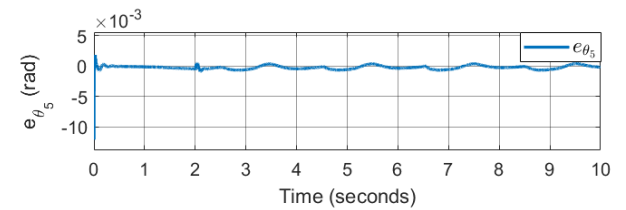
(b) Error of the second angle



(c) Error of the third angle



(d) Error of the fourth angle



(e) Error of the fifth angle

Figure 11: Error of the angles

The Fuzzy PID controller operates efficiently, reducing the error between the output values and the set values of the angular rotations to very low levels, below  $3.10^{-3}$ . When the robot starts moving, it takes approximately 0.4 seconds to stabilize along a straight trajectory, with the error between the x, y-axis trajectories and the set trajectory being only about 0.4 mm, indicating high accuracy in control and positioning. When switching to a curved trajectory, the errors of the axes increase to about 2.5 mm but remain within acceptable limits relative to the size of the robot.

#### 4.2. Tracking desired trajectory with disturbance

In this subsection, the control performance of the system under white noise is evaluated. The amplitude and frequency of the white noise, acting on joint  $q_5$ , is shown in Figure 12.

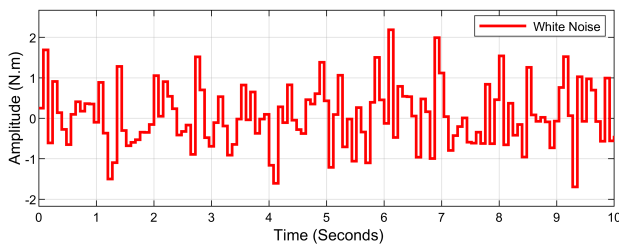


Figure 12: White noise on joint  $q_5$

Figure 13 provides the comparison of the actual and reference values for the end-effector.

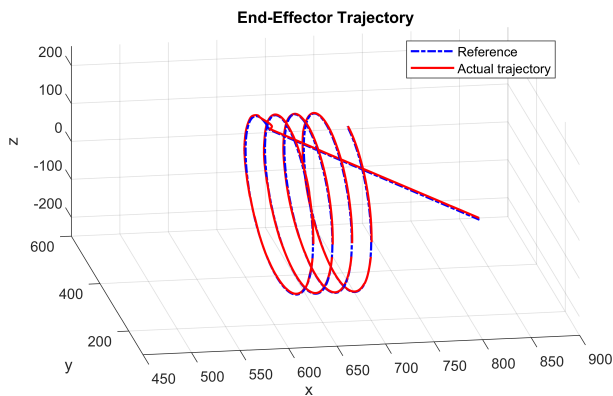


Figure 13: Comparison of actual and reference value for end-effector with white noise

Under the influence of white noise, the error results for the joints are presented in Figure 14. This graph should illustrate the error value comparison using Fuzzy PID controller and PID controller. This is demonstrated by the larger error magnitudes seen when disturbances are present, where the fixed parameters of the PID controller are unable to adjust to shifting circumstances, leading to less accuracy and more oscillations. On the other hand, handling such disturbances is much improved by the fuzzy PID controller. The fuzzy PID controller shows improved flexibility and resilience by using fuzzy logic to dynamically modify the control settings in response to real-time error and error rate data. This flexibility keeps things more closely aligned with the intended path by greatly reducing the impact of disruptions.

The end-effector error is shown in Figure 15, highlighting the

Table 8: RMS and Max errors for tracking with white noise

$e$	Max Error	RMSE
$e_{\theta_1} (rad)$	$8.654 \times 10^{-3}$	$1.086 \times 10^{-3}$
$e_{\theta_2} (rad)$	$6.862 \times 10^{-3}$	$3.495 \times 10^{-3}$
$e_{\theta_3} (rad)$	$9.010 \times 10^{-3}$	$1.599 \times 10^{-3}$
$e_{\theta_4} (rad)$	$2.700 \times 10^{-3}$	$9.259 \times 10^{-4}$
$e_{\theta_5} (rad)$	$1.209 \times 10^{-2}$	$1.235 \times 10^{-3}$
$e_{x-axis} (mm)$	3.410	$5.123 \times 10^{-1}$
$e_{y-axis} (mm)$	6.772	1.060
$e_{z-axis} (mm)$	4.708	2.371

extent to which the disturbance affects operational precision. A thorough assessment of the system's performance in the presence of white noise is provided by these error values, which show the differences between the actual and reference trajectories.

Table 8 summarizes the maximum error and RMSE for tracking under the influence of white noise, demonstrating high accuracy in angular tracking, with minimal angular errors. Notably,  $e_{\theta_4}$  exhibits a particularly low RMSE ( $9.259 \times 10^{-4}$  rad). While there is some deviation in positional tracking, these errors remain within manageable limits, with the x-axis showing the smallest maximum error (3.410 mm). These results indicate that the system effectively maintains precision in both angular and positional tracking, even in the presence of white noise.

The Fuzzy PID controller demonstrates effective performance even under the influence of white noise, with the errors in the joints remaining within acceptable limits. For the trajectories utilized in the simulation, which include two types of motion, the end-effector continues to closely follow the desired trajectory. The errors in the x, y, and z axes are comparable to those observed in the absence of noise, indicating that the controller maintains robust performance and accuracy despite the presence of disturbances.

## 5. Conclusion

This paper presents the implementation and evaluation of a Fuzzy PID controller for a 5-DoF robot, aimed at enhancing precision and stability in trajectory tracking tasks. The developed kinematic and dynamic models provide a comprehensive understanding of the robot's operational characteristics, including its dimensions, weight, joint angles, and maximum velocities. The Fuzzy PID controller, which dynamically adjusts control parameters, demonstrated significant improvements in the robot's performance across various scenarios. Simulation results show the controller's effectiveness in reducing angular and positional errors to very low levels, as well as achieving rapid stabilization along straight trajectories with minimal error. Even when following complex curved trajectories, the controller maintained performance within acceptable error limits. The system also exhibited robust and flexible performance under the influence of disturbances, such as white noise, further showcasing the controller's adaptability. These findings emphasize the potential of Fuzzy PID controllers in improving the precision and reliability of robotic systems, particularly for tasks that require high levels of accuracy and stability in dynamic environments.

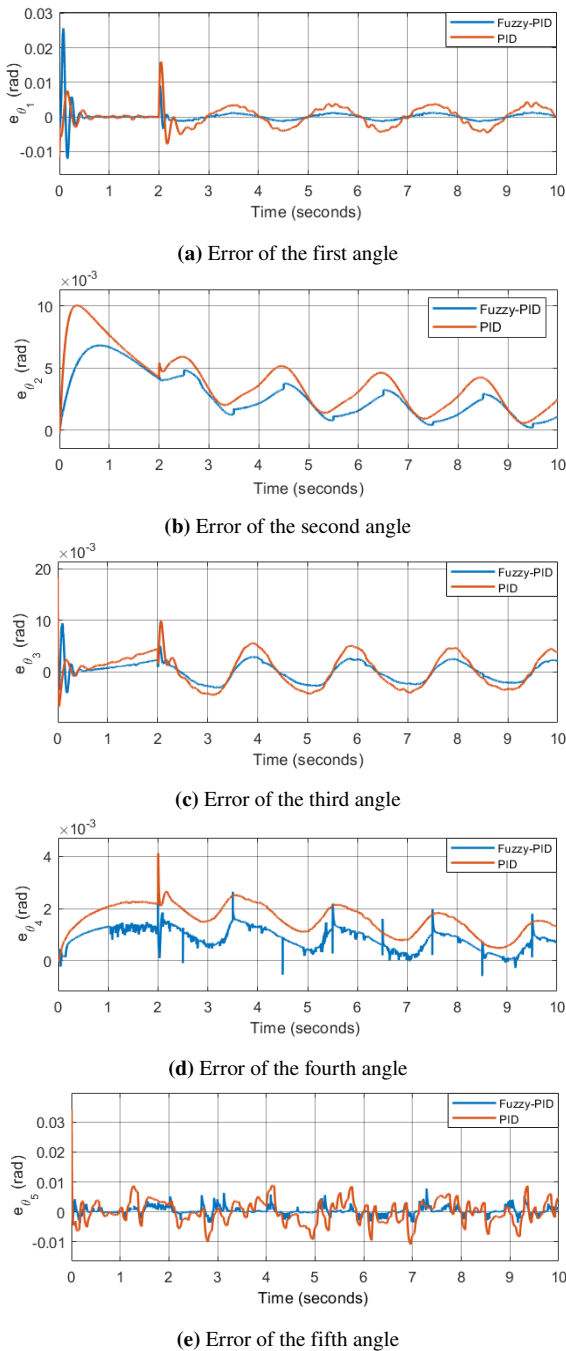


Figure 14: Error of the angles

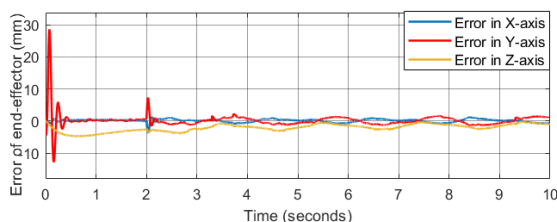


Figure 15: Error of end-effector

- [3] Benjamin Burger, Phillip M Maffettone, Vladimir V Gusev, Catherine M Aitchison, Yang Bai, Xiaoyan Wang, Xiaobo Li, Ben M Alston, Buyi Li, Rob Clowes, et al. A mobile robotic chemist. *Nature*, 583(7815):237–241, 2020.
- [4] Aude Billard and Danica Kragic. Trends and challenges in robot manipulation. *Science*, 364(6446):eaat8414, 2019.
- [5] Umme Zakia, Mehrdad Moallem, and Carlo Menon. PID-SMC controller for a 2-dof planar robot. In *2019 International Conference on Electrical, Computer and Communication Engineering (ECCE)*, pages 1–5. IEEE, 2019.
- [6] Mark W Spong, Seth Hutchinson, and Mathukumalli Vidyasagar. *Robot modeling and control*. John Wiley & Sons, 2020.
- [7] Saeed B Niku. *Introduction to robotics: analysis, control, applications*. John Wiley & Sons, 2020.
- [8] Yongyong Zhao, Jinghua Wang, Guohua Cao, Yi Yuan, Xu Yao, and Luqiang Qi. Intelligent control of multilegged robot smooth motion: a review. *IEEE Access*, 11:86645–86685, 2023.
- [9] Rakesh P Borase, DK Maghade, SY Sondkar, and SN Pawar. A review of pid control, tuning methods and applications. *International Journal of Dynamics and Control*, 9:818–827, 2021.
- [10] Jinke Zhang and Lei Guo. Theory and design of pid controller for nonlinear uncertain systems. *IEEE Control Systems Letters*, 3(3):643–648, 2019.
- [11] Junyoung Lee, Pyung Hun Chang, Byeonggi Yu, and Maolin Jin. An adaptive pid control for robot manipulators under substantial payload variations. *IEEE Access*, 8:162261–162270, 2020.
- [12] Phichitphon Chotikunnan and Rawiphon Chotikunnan. Dual design pid controller for robotic manipulator application. *Journal of Robotics and Control (JRC)*, 4(1):23–34, 2023.
- [13] Haibo Zhou, Rui Chen, Shun Zhou, and Zhenzhong Liu. Design and analysis of a drive system for a series manipulator based on orthogonal-fuzzy pid control. *Electronics*, 8(9):1051, 2019.
- [14] Claudio Urrea, John Kern, and Johanna Alvarado. Design and evaluation of a new fuzzy control algorithm applied to a manipulator robot. *Applied Sciences*, 10(21):7482, 2020.
- [15] Prasenjit Sarkhel, Nilotpal Banerjee, and Nirmal Baran Hui. Fuzzy logic-based tuning of pid controller to control flexible manipulators. *SN Applied Sciences*, 2:1–11, 2020.
- [16] Athar Ali, Syed Faiz Ahmed, Kushsairy A Kadir, M Kamran Joyo, and RN S Yarooq. Fuzzy pid controller for upper limb rehabilitation robotic system. In *2018 IEEE international conference on innovative research and development (ICIRD)*, pages 1–5. IEEE, 2018.
- [17] Edris Farah. Fuzzy pid based path tracking control of a 5-dof needle-holding robot. In *2017 International Conference on Communication, Control, Computing and Electronics Engineering (ICCCCEE)*, pages 1–5. IEEE, 2017.
- [18] GM Khoury, Maarouf Saad, Hadi Youssef Kanaan, and Claude Asmar. Fuzzy pid control of a five dof robot arm. *Journal of Intelligent and Robotic systems*, 40:299–320, 2004.
- [19] Meng Bi. Control of robot arm motion using trapezoid fuzzy two-degree-of-freedom pid algorithm. *Symmetry*, 12(4):665, 2020.
- [20] Reza Rouhi Ardeshiri, Hoda Nikkhal Kashani, and Atikeh Reza-Ahrabi. Design and simulation of self-tuning fractional order fuzzy pid controller for robotic manipulator. *International Journal of Automation and Control*, 13(5):595–618, 2019.
- [21] Cuiqiao Li, Ying Sun, Gongfa Li, Du Jiang, Haoyi Zhao, and Guozhang Jiang. Trajectory tracking of 4-dof assembly robot based on quantification factor and proportionality factor self-tuning fuzzy pid control. *International Journal of Wireless and Mobile Computing*, 18(4):361–370, 2020.
- [22] Abhishek Dhyani, Manoj Kumar Panda, and Bhola Jha. Design of an evolving fuzzy-pid controller for optimal trajectory control of a 7-dof redundant manipulator with prioritized sub-tasks. *Expert Systems with Applications*, 162:113021, 2020.

## References

- [1] Richard M Murray, Zexiang Li, and S Shankar Sastry. *A mathematical introduction to robotic manipulation*. CRC press, 2017.
- [2] Cristina Piazza, Giorgio Grioli, Manuel G Catalano, and Antonio Bicchi. A century of robotic hands. *Annual Review of Control, Robotics, and Autonomous Systems*, 2(1):1–32, 2019.